Kinetic roughening during rare-gas homoepitaxy

E. Nabighian,[1] M. C. Bartelt,[2] and X. D. Zhu[1,*]
[1]*Department of Physics, University of California, Davis, California 95616*
[2]*Sandia National Laboratories, Livermore, California 94550*
(Received 8 March 2000)

Using an optical-reflectivity-difference technique, we monitored the growth of multilayer Xe films on a commensurate monolayer of Xe on Ni(111) from 35 to 60 K. A transition occurs near 40 K from rough growth at low temperature to quasi-layer-by-layer growth characterized by persistent oscillations in the reflectivity difference. We discuss this transition in terms of changes in the island formation process and the onset of second-layer nucleation. The Xe sticking coefficient at 40 K is obtained from the period of the oscillations in the reflectivity difference. We find that the sticking coefficient decreases with increasing film thickness at fixed Xe pressure.

Epitaxial film growth far from thermodynamic equilibrium allows access to (often desired) stable structures and behaviors that would be typically impossible to realize near equilibrium. Refined understanding of the underlying atomic processes and of the influence of the surface geometry on growth structure has followed advances in scanning tunneling microscopy (STM), high-resolution electron and x-ray diffraction techniques, ion scattering, and, more recently, low-energy electron microscopy. In addition, lattice-gas models have been developed with a realistic description of deposition, surface diffusion, and island formation, and their behaviors matched to experiment using kinetic Monte Carlo simulation and analytical approaches.[1] Studies reveal that kinetic roughening, which accounts for deviations from layer-by-layer growth, is generally very sensitive to the strength of the barriers for downward transport at steps or island edges and to details of the deposition dynamics.[2] It also reflects the more subtle influence of equilibration or coarsening of surface features during growth.

Physisorbed layers of rare gases on metal surfaces are often considered simple model systems. This is so despite observations of complex adsorbate geometries, topological transitions controlled by strain, and the lack of a detailed understanding of the nature of the rare-gas bonds to most substrates; see e.g., Ref. 3. A quantitative assessment of the way in which rare-gas multilayer films roughen during growth is also not available.

Early experimental studies of submonolayer deposition of rare gases (Ar, Kr, and Xe) on graphite (0001) and amorphous carbon surfaces focused on wetting issues, melting, and structural phase transitions in the rare-gas overlayer.[4] A few studies examined island formation, including the dependence of the island density on deposition conditions, under normal vacuum ($>10^{-9}$ Torr).[5] Caution is justified when interpreting such data using classical nucleation theory. Nevertheless, the Arrhenius behavior of the island density between 30 and 60 K suggested a sequence of changes in island-nucleation parameters. The first for Xe in the above temperature (T) range was reported near 40 K, where a change in scaling of the island density with deposition flux was observed. However, on cleaner and better prepared graphite surfaces, step-flow growth of Xe films was reported, instead, near 50 K.[5]

Information on the growth of rare-gas films on metal substrates is even more limited. On Pt(111), deposited Xe atoms exhibit long-range transient motion and are able to form compact islands in registry with the substrate for T as low as 4 K.[6] Near $\frac{1}{3}$ of a monolayer (ML), the Xe adlayer is slightly buckled to relieve strain.[7] Denser monolayers of Xe/Pt(111), with ordered arrays of heavy domain walls, were reported before second-layer nucleation, but there is no evidence that this occurs on Ni(111). If common, these extended defects would certainly influence subsequent multilayer growth. Thicker Xe films have been reported to grow on Pt(111) in a quasi-layer-by-layer fashion below 40 K,[7] just as on Ag(111).[8]

Here, we study the growth of Xe films on Ni(111). Input parameters for analyses of the results, e.g., the barriers and prefactors for adatom diffusion on Xe terraces, across or along steps and around island corners are obtained (to a good approximation) from the Lennard-Jones-like form of the interactions between neighboring atoms; see Table I and Fig. 1. In these calculations, the Xe(111) substrate consists of three close-packed layers of atoms. The surface atoms are kept frozen, except during site exchange with an adatom.

We grew the Xe films in ultrahigh vacuum (base pressure $<5\times10^{-11}$ Torr) starting with a Ni(111) single-crystal surface, miscut by 0.1° (average terrace width of 900 Å). From the appearance of a sharp superlattice low-energy electron diffraction (LEED) pattern, we know that the first monolayer of Xe on Ni(111) forms a commensurate $(\sqrt{3}\times\sqrt{3})R30°$ structure, at an equivalent coverage of about 0.33 ML.[9] Below 60 K, the nearest-neighbor distance in this structure is the same as the Xe-Xe van der Waals separation, to within 1.4%. Consequently, the growth of subsequent layers of Xe, on which we focus here, takes place on this nearly stress-free Xe(111) ''substrate.'' The temperature was measured with a Chromel-Alumel thermocouple spot-welded to the side of the Ni(111) disk (1.2 cm in diameter). We studied growth between 35 and 60 K, above which desorption of Xe becomes significant. During growth, the Xe pressure was kept at 3.3×10^{-8} Torr. Under these conditions, the deposition flux was determined to be about 0.002 ML/s.

Growth of the Xe films was monitored with an oblique-incidence optical-reflectivity-difference technique.[9] As a probe, we used a 2-mW polarized He-Ne laser at an incidence angle of 66.5°. Let $r_{p0}=|r_{p0}|\exp(i\phi_{p0})$ and $r_{s0}=|r_{s0}|\exp(i\phi_{s0})$ denote the reflectivities for p- and s-polarized light from the substrate without the Xe overlayer,

TABLE I. Diffusion barriers (in meV) for Xe adatoms on Xe(111): E_d, on terraces; $E_e(A)$, (B) along A or B steps; E_c, around corners (hopping); $E_s(A,B)^{\mathrm{hop,ex}}$, down at A or B steps, via hopping (hop) or exchange (ex); $E_{sk}(A,B)$, down at kink sites on A and B steps; $E_{sc}(60°),(120°)$, down at 60° and 120° corners. ν is the attempt frequency (normal-mode frequencies at the $3fh$ site: 3.1, 1.4, and 1.4 THz; at the saddle point: 3.1 and 1.75 THz). The net change in binding energy upon separating one adatom (at a bond length of 4.34 Å) is $E_{1b}\approx 20$ meV from a dimer, $E_{2b}\approx 40$ meV$\approx 2E_{1b}$ from a compact trimer, and $E_{3b}\approx 60$ meV$\approx 3E_{1b}$ from a compact heptamer. They correspond to breaking single, double, and triple bonds, respectively. Note that $E_c < E_e(A)+(E_{2b}-E_{1b})$, due to interactions beyond nearest neighbors. We used $E\approx 0.08[(1.09r)^{-12}-(1.09r)^{-6}]$ for the potential energy (in eV) between pairs of Xe atoms at separation $R=rR_0$ (R_0 is the bulk Xe-Xe distance at 4 K$\approx$4.34 Å).

E_d	$E_e(A)$	$E_e(B)$	E_c	$E_s(A,B)^{\mathrm{hop}}$	$E_s(A,B)^{\mathrm{ex}}$	$E_{sk}(A,B)$	$E_{sc}(60°)$	$E_{sc}(120°)$	ν (THz)
8	42	21	52	33	53	28	33	35	1.1

and $rp=|r_p|\exp(i\phi_p)$ and $r_s=|r_s|\exp(i\phi_s)$ with the growing film. We define the reflectivity changes $\Delta_p=(r_p-r_{p0})/r_{p0}$ and $\Delta_s=(r_s-r_{s0})/r_{s0}$. In the experiment, we measured the imaginary part of the reflectivity difference, $\Delta_p-\Delta_s$, denoted by $\mathrm{Im}(\Delta_p-\Delta_s)$. This quantity follows the behavior of the dielectric constant of the overlayer, ϵ_0, and thus indirectly its roughness. For quasi-layer-by-layer growth, ϵ_0 (and thus $\Delta_p-\Delta_s$) oscillates with increasing film thickness, recovering to approximately the same value at each monolayer completion. For step-flow growth, ϵ_0 is independent of film thickness. For rough growth, ϵ_0 varies monotonically with thickness.

In Fig. 2 we show the observed change in $\mathrm{Im}(\Delta_p-\Delta_s)$ for increasing Xe dosage (in langmuirs or L, 1 L$=10^{-6}$ Torr s), at 35 and 40 K. Behavior at other T in this range interpolates smoothly between the curves shown. At 40 K, $\mathrm{Im}(\Delta_p-\Delta_s)$ increases from zero to 3.3×10^{-3} monotonically up to a dosage of 15 L ($\approx$3 ML), and then oscillates with additional Xe dosage. The amplitude of the oscillations is roughly 10^{-3}, undamped for several oscillations. In contrast, at 35 K, $\mathrm{Im}(\Delta_p-\Delta_s)$ increases monotonically with increasing Xe dosage, a signature of rough growth. From 40 to 60 K, the variation of $\mathrm{Im}(\Delta_p-\Delta_s)$ with Xe dosage is qualitatively similar, consistent with quasi-layer-by-layer growth. Near and above 60 K, the film interface roughens due to significant Xe desorption during growth, producing rapid decay of the oscillations in $\mathrm{Im}(\Delta_p-\Delta_s)$ (data not shown).

The oscillatory behavior of $\mathrm{Im}(\Delta_p-\Delta_s)$ at 40 K can be qualitatively understood by noting that $\Delta_p-\Delta_s$ is proportional to the difference in the optical response of fully coordinated and undercoordinated Xe atoms. During quasi-layer-by-layer growth, the density of these undercoordinated atoms (with less than six nearest neighbors in the surface plane) first increases, as new islands nucleate on terraces. Thus, $\mathrm{Im}(\Delta_p-\Delta_s)$ increases accordingly. Subsequent deposition leads to island growth and coalescence, which reduces the surface density of under-coordinated atoms. Thus, $\mathrm{Im}(\Delta_p-\Delta_s)$ decreases towards completion of the monolayer. This behavior of $\mathrm{Im}(\Delta_p-\Delta_s)$ is repeated for successive monolayers. The monotonic increase in $\mathrm{Im}(\Delta_p-\Delta_s)$ at low T is then simply attributed to a continued increase in the density of undercoordinated Xe atoms at the film interface.

The oscillations in $\mathrm{Im}(\Delta_p-\Delta_s)$ were used to estimate the actual deposition flux ($\approx$0.002 ML/s) and, in comparison with the known Xe dosage, to extract an effective sticking coefficient S for impinging Xe atoms. The inset in Fig. 2 reveals that S decreases rapidly with increasing film thickness. To understand this behavior, note that S should be generally sensitive to the efficiency of the atomic mechanisms by which kinetic energy and momentum normal to the surface are transferred from the arriving atoms to the surface.[10] This occurs primarily via surface phonons in the case of rare gases. Both the mass misfit between impinging and surface atoms and their relative binding energy are important factors. The latter can be stronger near the metallic substrate, since additional polarization effects are possible, but momentum transfer to the substrate will be more efficient the lighter the substrate atoms relative to the rare gas. The net effect on S can be nontrivial. For Ar/Ru(001), with a mass ratio of 0.4, S first increases as the area of bare substrate decreases and then gradually saturates by 2 ML.[11] For Xe/Ni(111), with a mass ratio of 2.4, both the mass and the binding energy factors argue for a decrease in S with increasing film thickness. Xe

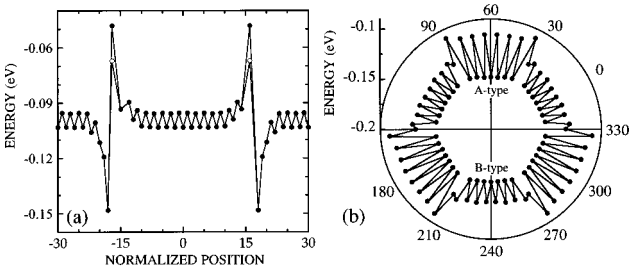

FIG. 1. Energy of a Xe adatom (a) along a diffusion path on a Xe(111) terrace and across a step edge, and (b) along the perimeter of a hexagonal island with alternating A- and B-type steps. The adatom position is in units of the lattice constant. Solid circles: diffusion via exchange; open circles: via hopping. In (a), note that the binding energy at a threefold-hollow site at a step edge is smaller than on a terrace, due to additional next-nearest-neighbor interactions in the latter.

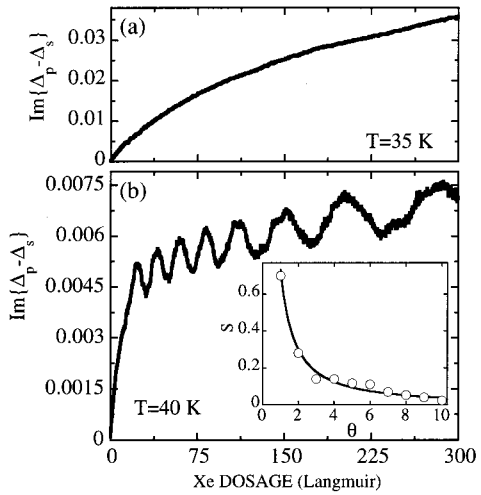

FIG. 2. The measured $\mathrm{Im}(\Delta_p-\Delta_s)$ vs Xe dosage, at (a) 35 K and (b) 40 K. The change in $\mathrm{Im}(\Delta_p-\Delta_s)$ is 0.0013 for 1 ML of Xe on Ni(111). Inset: S (at 40 K and fixed Xe pressure) vs the number θ of Xe monolayers. The solid line is the fit $S=0.7\theta^{-1.3}$.

atoms are less likely to ''bounce'' off Ni and as a result, they are in longer contact, thus making S the largest for the first monolayer of Xe.

We now discuss several transitions that might account for the crossover in growth mode observed near 40 K. We base this discussion on the energy barriers listed in Table I and on the generic behavior of lattice-gas models of film growth during deposition. We caution, however, that slight deviations in the energy barriers can shift quantities significantly. Such deviations could arise for films of a few monolayers due to longer-range effects mediated by the Ni substrate (or due to impurities, like H).

(i) Transitions in critical island size and the onset of second layer nucleation. Transitions in island nucleation parameters, e.g., from irreversible to reversible island nucleation, will affect the onset of second-layer population, and thus the kinetic roughening behavior. For a fcc(111) system with sufficiently strong nearest-neighbor pairwise adatom interactions, one expects a gradual transition with increasing T from $i=1$ (all islands are effectively stable) to $i=2$ (doubly-bonded configurations such as compact trimers are stable) when $Y=(h/F)\exp[-3E_{1b}/(2k_BT)]\approx O(1)$.[12] Here, $h=\nu\exp(-Ed/(k_BT))$ is the adatom hopping rate, F is the deposition flux, and E_{1b} is the binding energy of an addimer. Another transition occurs at higher T, from $i=2$ to $i=6$ (triply bonded configurations such as compact septamers are stable) when $Y=(h/F)\exp[-3E_{2b}/(2k_BT)]\approx O(1)$, with $E_{2b}\approx 2E_{1b}$.[12] For the parameters in Table I, we find $T_{i=1\to 2}\approx 13$ K and $T_{i=2\to 6}\approx 23$ K, suggesting that the major transitions in i occur below the range of T of our study.

As a measure of the propensity to deviate from layer-by-layer growth (i.e., to start a layer before the previous is completed), we examine the probability $P(R)$ of nucleating islands on top of an island of radius R. $P(R)$ is significant for islands of radius above a certain value R_c. R_c depends on i and on the diffusion rates on top (h_d) and down $h'=\nu\exp(-E_d+E_s)/(k_BT)$ at the edge of islands (see Table I). These parameters also control the average island radius $R_{\rm av}$. The exact dependence of P on R is illustrated in Fig. 3, for island distributions obtained at fixed coverage from simulations of irreversible ($i=1$) island formation in each layer.[2] Behavior of P for $i>1$ is qualitatively similar. In particular, R_c and $R_{\rm av}$ increase with increasing h/F and h'/h, and different scaling forms, $P(R/R_c)$, apply for small and large h'/h (or, better, for small and large $R_c/R_{\rm av}$).

A rate-equation analysis[13] for general i and a single circular island of radius $R_{\rm av}$, or a sharp distribution of radii about $R_{\rm av}$, obtained $P(R_{\rm av})=1-\exp[-(R_{\rm av}/R_c)^{\sigma}]$. Here, $\sigma=2i+6$ and $R_c\approx R_{\rm av}\sim\{(h/F)^i\exp[-E_i/(k_BT)]\}^{1/(2i+4)}$, for small $\Gamma=E_S/E_d$; $E_i>0$ is the binding energy for islands of size i (so $E_1=0$, $E_2=E_{1b}$, etc.). For large Γ, $\sigma=i+5$ and $R_c\approx[R_{\rm av}^{2i+6}L_{\rm SE}^{-(i+1)}]^{1/\sigma}$, with $L_{\rm SE}=\exp[E_S/(k_BT)]=h/h'$. Figure 3 shows that the rate-equation form provides a fairly good description of the transition region, $R=R_c$, for $i=1$. Presumably this applies also for $i>1$.

In practice, the important parameter is the ratio $R_c/R_{\rm av}$: if it is sufficiently large, then growth is smooth. Using Xe parameters (Table I), we find $R_{\rm av}(40\,{\rm K})/R_{\rm av}(35\,{\rm K})\approx O(1)$, so in order to elucidate the difference in growth mode between 35 and 40 K, we need only compare the R_c values. For large

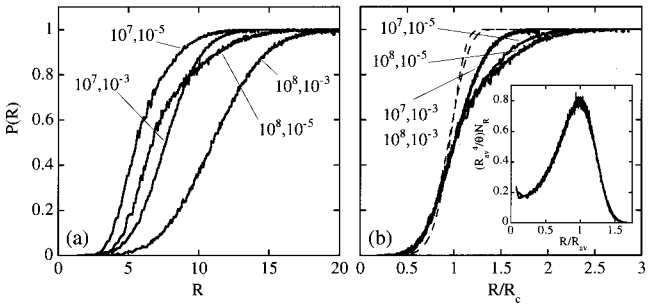

FIG. 3. Simulation results for $P(R)$ at 0.5 ML (1200×1200 site lattices; 500 runs), in (a) versus R (in atoms) and in (b) versus R/R_c. R_c is defined as $P(R_c)\approx\frac{1}{2}$. Data shown are for compact islands formed irreversibly, using different $(h/F,h'/h)$ pairs, as indicated: $h/F=10^7$, $h'/h=10^{-5}$ ($R_{\rm av}\approx 8.8$, $R_c\approx 5.5$, $R_c/R_{\rm av}\approx 0.62$; rms film roughness $W\approx 0.650$) and $h'/h=10^{-3}$ ($R_{\rm av}\approx 9.0$, $R_c\approx 7.6$, $R_c/R_{av}\approx 0.84$, $W\approx 0.624$); and $h/F=10^8$, $h'/h=10^{-5}$ ($R_{\rm av}\approx 12.7$, $R_c\approx 6.7$, $R_c/R_{\rm av}\approx 0.53$, $W\approx 0.663$) and $h'/h=10^{-3}$ ($R_{\rm av}\approx 13.0$, $R_c\approx 11.0$, $R_c/R_{\rm av}\approx 0.84$, $W\approx 0.626$). The form $P(R)=1-\exp[-(R/R_c)^{\sigma}]$, with $\sigma=8(6)$ for small (large) h'/h, in dashed lines, deviates from the exact behavior for $R>R_c$ but describes fairly well the transition region. Deviations reflect the nontrivial form of the distribution of first-layer island radii, N_R (inset).

$\Gamma\approx 4$ (Table I) the rate-equation analysis predicts $1<R_c(40\,{\rm K})/R_c(35\,{\rm K})<10$, for $1\leqslant i\leqslant 6$, with a higher ratio the larger the i. Since i is at least 6 for Xe/Xe(111) at 35–40 K, this result explains the observed smoother growth at 40 K. Simulation results reveal more complex scaling behavior of R_c, e.g., $R_c\propto L_{\rm SE}^{-i/(3i+4)}$ for large Γ,[14] but one still finds $R_c(40\,{\rm K})/R_c(35\,{\rm K})\approx O(10)$ for $i=6$ using the Xe parameters.

(ii) Transition to step-flow growth. It is pertinent, especially for low-corrugation surfaces, to compare the anticipated characteristic separation between islands, L, with the average terrace width, L_t. Step-flow growth occurs if $L\gg L_t$. To estimate L for a clean surface, the key parameter is the ratio h/F. Between 35 and 60 K, one gets $h/F>10^{12}$ using E_d and ν from Table I and $F\approx 0.002$ ML/s. Therefore, $L>500$ Å, for all $i\geqslant 1$, based on simulation results.[15] Although more islands than average form near descending steps when the step-edge barriers are large, as for Xe/Xe(111), our $L_t\approx 900$ Å is sufficiently close to L that one should observe step-flow growth at least for the thicker films. However, even minute concentrations of defects will provide sites for heterogeneous island nucleation, thereby delaying the transition to step-flow growth.

(iii) Transitions in island shape. Island shapes are important to kinetic roughening behavior, since the step-edge barriers can depend strongly on the atomic structure of the edges. An estimate of the range of T where transitions in island shape might occur in our system, can be obtained by comparing the time τ_a between successive aggregation events of diffusing adatoms with islands to the time scale τ_e, for island shape equilibration.[16] If $\tau_a<\tau_e$, then island shape instabilities will develop, i.e., ramified islands form. Given the island density N (per adsorption site), one has $\tau_a=N/F\ll 1/F$. Island-perimeter diffusion dominates the shape-equilibration process at low T, and since $E_e<E_c$, τ_e is in fact controlled by the rate of corner crossing, so $1/\tau_e\sim\nu\exp[-E_c/(k_BT)]$. A weak criterion for shape instabilities is then $\tau_e>1/F$, or $T<T_c\approx 28$ K for $F\approx 0.002$ ML/s and $\nu\approx 1$ THz. So, islands would develop a ramified shape below 28 K but a compact shape above. The actual T_c will be larger

(since $N \ll 1$), possibly falling above 35 K. Since ramified island shapes assist layer-by-layer growth, a transition to a compact shape with increasing T is probably not so relevant to understand the difference in growth mode between 35 and 40 K.

On the basis of our data, we cannot discount the occurrence of more than one of these transitions in our films in the range of T of our study. However, short of an exotic change in the nature of the island nucleation process, it appears that a significant increase in R_c from 35 to 40 K (due to large i) can completely account for the observed transition to quasi-layer-by-layer growth at 40 K.

Finally, we explore the effect of a thickness-dependent Xe sticking coefficient on the film structure. For this purpose, we performed simulations with S varying as in Fig. 2 and monitored the dependence of the surface step density, $N_{\rm sd} \propto \mathrm{Im}(\Delta_p - \Delta_s)$, on film thickness. Results are shown in Fig. 4. For small h'/h and fixed h/F, the film roughens without lasting oscillations, as for the Xe system at the lower T. However, even a small shift in h'/h from 0.1 to 0.5 produces strong oscillations in $N_{\rm sd}$, characteristic of layer-by-layer growth. There is also the possibility that h and h' change with increasing film thickness, corresponding to changes in the barriers for adatom diffusion with increasing distance from the Ni substrate. For the parameters that we tested, this only affected the value of $N_{\rm sd}$ and the amplitude of the oscillations, not their period.

In summary, at Xe pressures of 3×10^{-8} Torr, Xe/Xe/Ni(111) films grow very rough below 40 K and above 60 K but quasi-layer-by-layer between 40 and 60 K. Rough growth at low T is likely controlled by large effective barriers for downward diffusion at the edge of compact islands. The crossover to smooth growth at 40 K is consistent with a tenfold increase in the critical island radius for second-layer nucleation. If the parameters in Table I are fairly accurate, then it is conceivable that island nucleation is not homogeneous at or above 40 K. Thus, we are currently examining the sensitivity of growth behavior on the density of defects and impurities deliberately introduced in the Xe/Ni system.

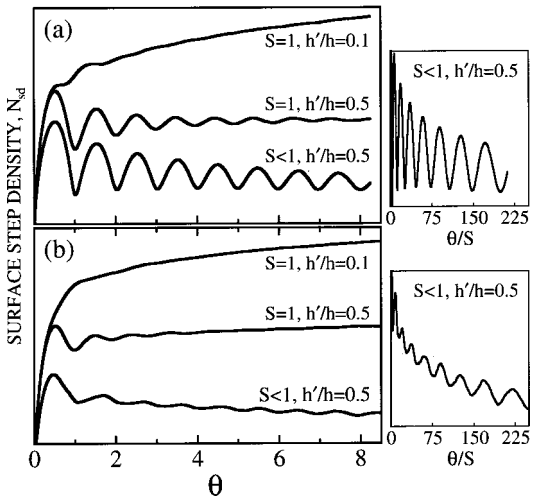

FIG. 4. Simulation results for N_{sd} (in arbitrary units) versus coverage θ (in ML). The insets show N_{sd} vs dosage θ/S. In (a) we used $h/F=10^8$ (Ref. 17) and compare results for different S and h'/h, for growth on a singular surface (500×500 site lattices). $S<1$ means $S=0.7\theta^{-1.3}$. The shift in the position of the minima below $\frac{1}{2}$, monolayers. for small h'/h, reflects a skewed distribution of surface heights (Ref. 2). Growth is smoother for $S<1$ (at fixed h/F and h'), as expected. In (b), we used $h/F=10^6$ for growth on a miscut surface ($L/L_t \leqslant 0.07$).

This work was supported by the Petroleum Research Fund of the American Chemical Society and by the National Science Foundation under Grant No. DMR-9818483 (X.D.Z.). M.C.B. is supported by the Office of Basic Energy Sciences, Division of Materials Sciences, of the U.S. DOE, under Contract No. DE-AC04-94AL85000.

*Corresponding author. E mail: xdzhu@physics.ucdavis.edu

[1] H. Brune, Surf. Sci. Rep. **31**, 121 (1998); J. W. Evans, M. C. Bartelt, and P. A. Thiel (unpublished).

[2] M. C. Bartelt and J. W. Evans, Phys. Rev. Lett. **75**, 4250 (1995); Surf. Sci. **423**, 189 (1999).

[3] K. Kern *et al.*, Phys. Rev. Lett. **56**, 620 (1986); Surf. Sci. **195**, 353 (1988).

[4] H. S. Youn *et al.*, Phys. Rev. B **48**, 14 556 (1993).

[5] J. A. Venables and D. J. Ball, Proc. R. Soc. London, Ser. A **322**, 331 (1971); G. L. Price and J. A. Venables, Surf. Sci. **49**, 264 (1975).

[6] P. S. Weiss and D. M. Eigler, Phys. Rev. Lett. **69**, 2240 (1992).

[7] K. Kern *et al.*, Phys. Rev. Lett. **56**, 2823 (1986); Solid State Commun. **62**, 391 (1987).

[8] A. Itakura and I. Arakawa, J. Vac. Sci. Technol. A **9**, 1779 (1991); S. Igarashi *et al.*, *ibid.* **16**, 974 (1998); J. Unguris *et al.*, Surf. Sci. **87**, 415 (1979); **87**, 437 (1979); **109**, 522 (1981); **114**, 219 (1982); R. J. Behm *et al.*, J. Chem. Phys. **85**, 1061 (1986).

[9] A. Wong and X. D. Zhu, Appl. Phys. A: Mater. Sci. Process. **63**, 1 (1996).

[10] H. Schlichting *et al.*, J. Chem. Phys. **97**, 4453 (1992).

[11] M. Head-Gordon and J. C. Tully, J. Chem. Phys. **95**, 9266 (1991).

[12] A transition in the size i, above which islands are effectively stable against dissociation during deposition, is naturally described in terms of the ratio, $\lambda = H_{\rm diss}/H_{\rm agg}$, of the rate at which islands of size $i+1$ dissociate, $H_{\rm diss} \propto \exp[-E_{ib}/(k_BT)]h$, to the rate at which adatoms of density n and diffusion rate $h = \nu \exp[-E_d/(k_BT)]$ aggregate with these islands $H_{\rm agg} \propto hn$. k_B is the Boltzmann constant. A transition is expected for $\lambda \approx O(1)$. In the steady state, where $n \propto F/(hN)$ and $N \propto (h/F)^{i/(i+2)} \exp[-E_{ib}/(i+2)(k_BT)]$ is the average island density, λ depends only on $Y_1 = (h/F)\exp[-3E_{1b}/(2k_BT)]$, for transitions out of $i=1$, and on $Y_i = (h/F)\exp[-(i+1)E_{ib}/(2k_BT)]$, for transitions out of $i>1$. Once triple bonds can dissociate on the time scale of deposition (so $i>6$), then all islands are unstable (in the absence of strong bonds beyond nearest neighbors), and a formulation based on a sharp value of i is less useful. See M. C. Bartelt, L. S. Perkins, and J. W. Evans, Surf. Sci. **344**, L1193 (1995).

[13] J. Tersoff *et al.*, Phys. Rev. Lett. **72**, 266 (1994).

[14] J. Rottler and P. Maass, Phys. Rev. Lett. **83**, 3490 (1999).

[15] J. W. Evans and M. C. Bartelt, J. Vac. Sci. Technol. A **12**, 1800 (1994); J. G. Amar and F. Family, Phys. Rev. Lett. **74**, 2066 (1995).

[16] Y. Li *et al.*, Phys. Rev. B **56**, 12 539 (1997).

[17] Corresponding behavior for the Xe parameters in Table I, e.g., $h/F \approx 10^{14}$ and $h'/h \approx 10^{-4}$ at 40 K, should be similar, but simulations would be much more time consuming.